

## ACKNOWLEDGMENTS

This work is partly supported by Hong Kong Polytechnic University under research grant no. G-T227 and by the Zhejiang Province Natural Science Foundation under grant no. M603085.

## REFERENCES

1. M. Schell, D. Huhse, A.G. Weber, G. Fischbeck, D. Bimberg, D.S. Tarasov, A.V. Gorbachov, and D.Z. Gorbuzov, 20-nm wavelength tunable single-mode picosecond pulse generation at 1.3  $\mu\text{m}$  by self-seeded gain-switched semiconductor laser, *Electron Lett* 28 (1992), 2154–2155.
2. S. Li, K.T. Chan, and C. Lou, Wavelength-tunable picosecond pulses generated from stable self-seeded gain-switched laser diode with linearly chirped fibre Bragg grating, *Electron Lett* 34 (1998), 1234–1236.
3. K. Chan and C. Shu, Electrically wavelength-tunable picosecond pulses generated from a self-seeded laser diode using a compensated dispersion-tuning approach, *IEEE Photon Technol Lett* 11 (1999), 1093–1095.
4. J.W. Chen, D.N. Wang, W. Jin, and Z.N. Li, Differential absorption measurement by use of self-seeded gain-switched Fabry-Perot laser diode, *Electron Lett* 38 (2002), 1434–1435.
5. L.P. Barry and P. Anandarajah, Effect of side-mode suppression ratio on the performance of self-seeded gain-switched optical pulses in light-wave communications systems, *IEEE Photon Technol Lett* 11 (1999), 1360–1362.
6. J.W. Chen and D.N. Wang, Self-seeded, gain-switched optical short pulse generation with high sidemode suppression ratio and extended wavelength-tuning range, *Electron Lett* 39 (2003), 679–681.
7. S. Li, K.S. Chiang, W.A. Gambling, Y. Liu, L. Zhang, and I. Bennion, Self-seeding of Fabry-Perot laser diode for generating wavelength-tunable chirp-compensated single-mode pulses with high-sidemode suppression ratio, *IEEE Photon Technol Lett* 12 (2000), 1441–1443.

© 2005 Wiley Periodicals, Inc.

## DESIGN OF A NOVEL MICROSTRIP ELECTROMAGNETIC BANDGAP (EBG) STRUCTURE

Gonca Çakır<sup>1</sup> and Levent Sevgi<sup>2</sup>

<sup>1</sup> Department of Electronics and Communication Engineering  
Kocaeli University  
Kocaeli, Turkey

<sup>2</sup> Department of Electronics and Communication Engineering  
Doğuş University  
Zeamet Sokak, No 21  
Acibadem, Istanbul, Turkey

Received 22 February 2005

**ABSTRACT:** This paper presents the design, simulation, and experimentation of a novel low-cost small-size high-performance microstrip (MS) electromagnetic bandgap (EBG) structure for MIMIC applications. The simulations and measurements confirm that the stopband characteristics can be easily controlled by changing the stub lengths and the interstub gap. © 2005 Wiley Periodicals, Inc. *Microwave Opt Technol Lett* 46: 399–401, 2005; Published online in Wiley InterScience (www.interscience.wiley.com). DOI 10.1002/mop.20999

**Key words:** microstrip line; planar bandstop filter; electromagnetic bandgap (EBG); FDTD; Chebyshev filter

## 1. INTRODUCTION

Photonic bandgap (PBG) structures have increasingly gained attention in electromagnetics (EM) and optics during the last decade for systems associated with communications, data storage, and

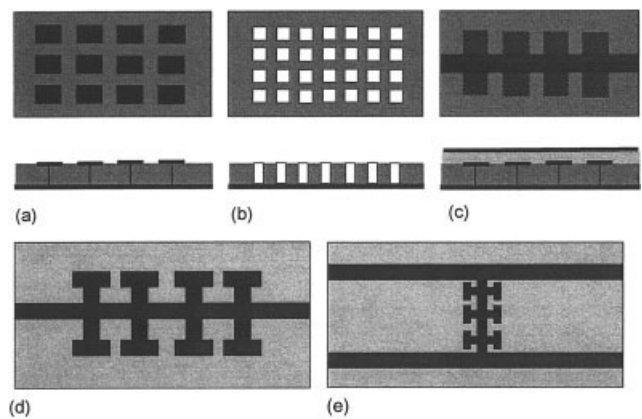


**Figure 1** Different microstrip EBG and EBS structures; (a) ground-wired small patched EBG; (b) air- or dielectric-dipped EBG; (c) three-layer ground-wired small patched EBG; (d) an application of EBS; (e) an application of EBG

computing [1–4]. Following the photonic bandgap (PBG) in optics [1], EBG terminology was first proposed in [5], and since then a variety of EBG forms [6], such as dielectric rods or holes, mushroomlike EBG structures, and even woodpile EBG materials [7], have been used in the microwave region, for example, to improve the radiation and beam-steering characteristics of antennas [8], to achieve high-performance filters, to act as an artificial magnetic conductor (AMC) [9], to form frequency selective surfaces, and to design power dividers, couplers, and so forth.

Planar EBG structures have attracted significant interest in microwave and MMIC applications due to their simplicity in manufacturing and ease of monolithical integration with other

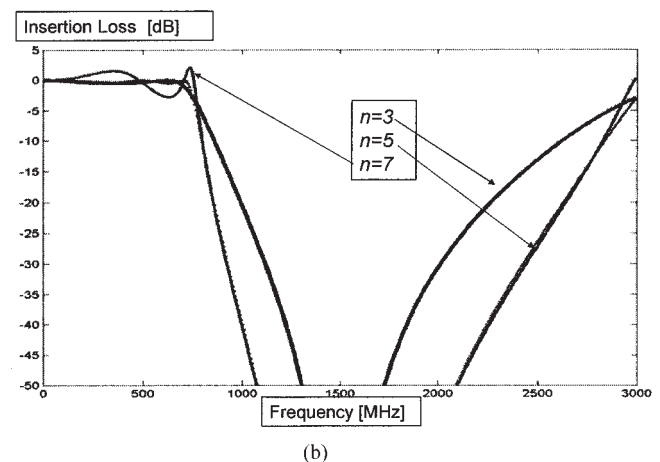
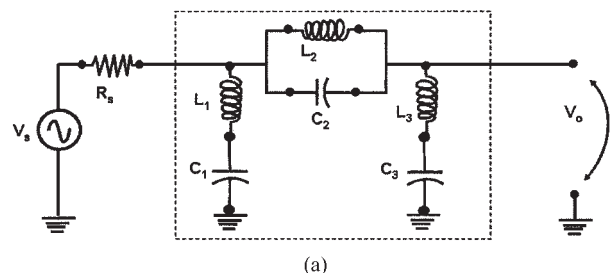


**Figure 2** (a) Circuit equivalent of the proposed bandstop structure (a 3<sup>rd</sup>-order bandstop Chebyshev filter); (b) Insertion loss vs. frequency for ( $n = 3, 5,$  and  $7$ )

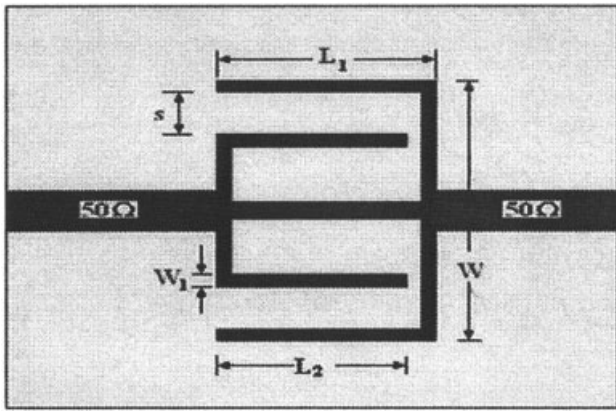


**Figure 3** The proposed microstrip structure having bandstop characteristics ( $W = 25$  mm,  $L_1 = 30$  mm,  $W_1 = 1$  mm,  $L_2 = 27$  mm,  $s = 5$  mm)

circuits. Their applications have been extended to a wide frequency range, even to microwave and millimeter-wave ranges. EM bandgap (EBG) structures are either etched directly onto the microstrip (MS) lines or immersed in the dielectric substrates. It is possible to control and manipulate the flow of EM fields by using EBG structures. Periodic metallization in the dielectric substrate behaves as a stop-band filter, which makes them suitable for surface current/wave (that is, noise and interference) reduction.

An EBG structure is nothing but an EM bandstop (EBS) filter, and a debate over the terminology of these structures has continued. Actually, the difference between them is not their structures, but their application. In Figure 1, several types of two- and three-layer MS EBG and EBS structures are shown. These types of EBG structures are generally inserted indirectly in the circuit in order to eliminate unwanted interference or noise effects in a certain frequency band. The first three structures [Figs. 1(a) to 1(c)] are examples of EBS structures. Figures 1(d) and 1(e) are examples of EBS and EBG applications, respectively.

In this paper, a novel compact bandstop filter is proposed that can be used either in EBG or EBS applications. Firstly, analog filter design principles are used to understand and create the MS structure that is expected to suppress certain signals in a given frequency band. Then, the MS structure is introduced, its characteristics are analyzed using the FDTD-based M-PATCH package

[10, 11], and the dimensions are optimized. Finally, the scattering parameters of the structure are measured. The presented structure is more compact than some of the previously proposed MS structures (for example, see [12]).

## 2. CLASSICAL CHEBYCHEV-TYPE BANDSTOP FILTER

Chebyshev filters are used when steeper descent (in attenuation) beyond the passband is required, at the cost of a permissible ripple in the passband [13]. The design parameters are the maximum permissible ripple in the passband and the attenuation at a given frequency beyond the passband (which determines the descent rate), from which the order of the filter can be extracted. The standard design prototype is the lowpass (LP) filter, and the other prototypes—highpass (HP), bandpass (BP), and bandstop (BS) filters—can be derived from this LP design.

The design parameters are chosen as follows in this paper: the center frequency of the stopband is 1.5 GHz, and the 3-dB and 40-dB bandwidths are 1 GHz and 500 MHz, respectively. This necessitates a 3<sup>rd</sup>-order Chebyshev filter [13], as shown in Figure 2(a), with actual element values of  $C_1 = 5.933$  pF,  $L_1 = 1.897$  nH,  $C_2 = 1.100$  pF,  $L_2 = 10.186$  nH, and  $C_3 = 5.837$  pF,  $L_3 = 1928$  nH for 50 $\Omega$  source and load impedances. The insertion loss of this filter is given in Figure 2(b). The 5<sup>th</sup>- and 7<sup>th</sup>-order filter responses are also plotted in Figure 2(b). As observed, the 3<sup>rd</sup>-order filter satisfies the design requirements, and one may choose higher-order filters if a steeper suppression ratio is required outside the band, at the cost of a higher ripple in the band.

## 3. DESIGN OF A NOVEL MICROSTRIP EBG STRUCTURE

A parallel LC-resonant circuit inserted serially (or, a series-resonant circuit inserted in parallel) between the input and output behaves as a band-stop filter. These form the basics of the proposed structure which, may also be the generic cell of an EBG (see Fig. 3). The structure is composed of two slot-etched (L-shaped) stubs on the MS rectangular patch. The two L-shaped stubs, one in the vicinity of the other, on both sides of the main line act as two parallel LC circuits with two different resonance frequencies, and are capacitively coupled to each other so as to obtain broad and clean stop-band characteristics. The input/output loads are achieved via tapped feed lines of 50 $\Omega$ . The substrate has relative dielectric constant of  $\epsilon_r = 2.4$  and thickness of  $h = 1$  mm. The other dimensions are optimized according to the design require-

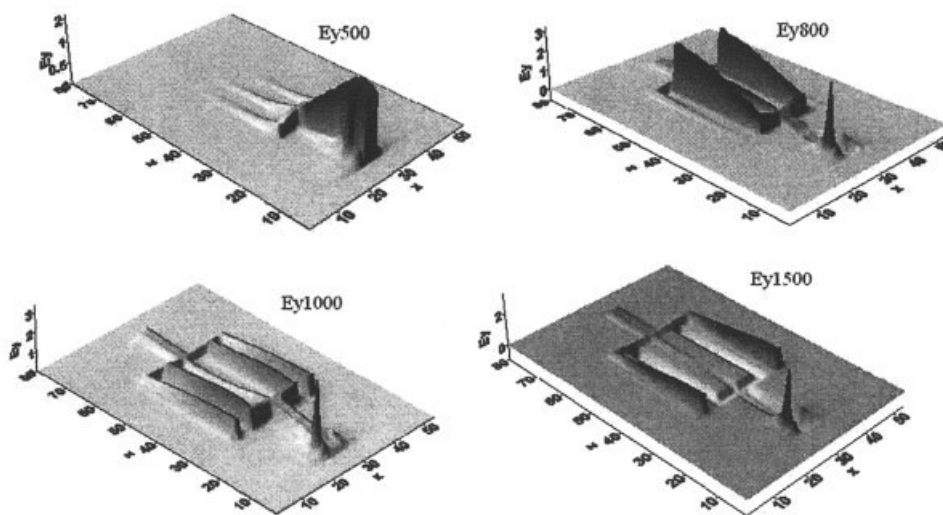


**Figure 4** Three-dimensional plots at different time instants recorded during the FDTD simulations

ments via several simulation trials using the FDTD-based M-PATCH package.

To ensure the required accuracy in the simulations, the FDTD cell size is chosen to be less than a  $1/20$  wavelength at the maximum frequency of interest (cell sizes are  $\Delta x = \Delta y = \Delta z = 1$  mm). The FDTD computation volume is  $55\Delta x \times 20\Delta y \times 81\Delta z$ . An eight-layer perfectly matched layer (PML) termination is used, which yields relative artificial reflections less than  $10^{-5}$ . The optimization results in dimensions of  $W = 25$  mm,  $L_1 = 30$  mm,  $W_1 = 1$  mm,  $L_2 = 27$  mm, and  $s = 5$  mm. In Figure 4, FDTD simulated transient responses at different time instants are shown for the visualization of broadband EM scattering along the structure, where one can trace the propagation along the line, the wave coupling to the stubs, and multireflections. From these time-domain responses, the broadband-frequency responses are calculated via offline discrete Fourier transformation (DFT).

The scattering parameters for the proposed structure are measured using an Agilent-8714 ES network analyzer. The frequency characteristics of the novel structure, obtained via the FDTD simulations and the measurements, are plotted in Figure 5. The response of the 3<sup>rd</sup>-order Chebychev filter is also given in the figure. Very good agreement among the results shows the strength of the design approach applied in this paper. The simulation tests are also performed to analyze effects of some of the geometrical parameters, such as the slot width  $s$  and the patch length  $L_1$ . These tests show that (i) as the slot width increases, the stopband width decreases and (ii) the center frequency of the stopband is inversely proportional with the length  $L_1$ .

To show the compactness of the presented EBG structure, a comparison with an example from the literature [13] is given in Figure 6. Here, the dimensions of the presented structure are rescaled accordingly in order to meet the design parameters of [13] (center frequency = 8 GHz,  $\epsilon_r = 10.2$ ,  $h = 0.4$  mm). As observed, a better bandstop performance is obtained with smaller (by approximately 30%) dimensions when the presented structure is used.

#### 4. CONCLUSION

A novel MS structure that can be used as either an EBG or EBS filter has been proposed and analyzed in this paper. Analog filter approaches were initially used to create the shape of the MS structure, and then optimized by means of a full-capable simulator based on the 3D-FDTD method. The structure was also fabricated and measured for validation purposes. It was demonstrated that the

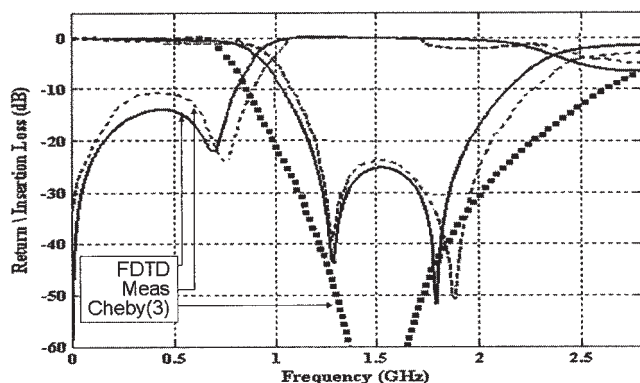


**Figure 5** Insertion loss vs. frequency for the microstrip EBG structure (solid line: FDTD simulations, dashed line: measurements; dotted line: 3<sup>rd</sup>-order analog filter response)

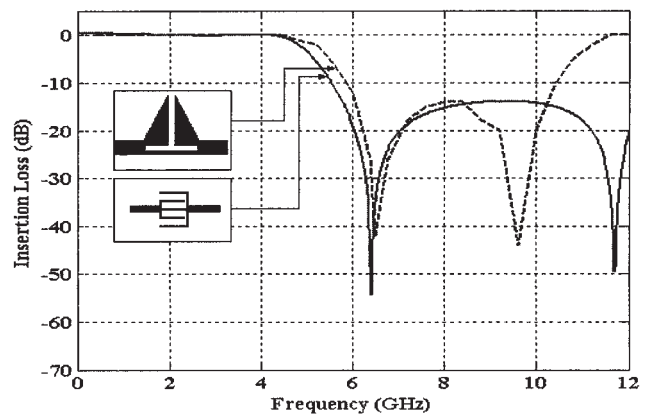


**Figure 6** Comparison of insertion loss vs. frequency for the presented EBG structure with the one in [13]

stopband characteristics can flexibly be controlled by changing the critical dimensions of the structure.

#### REFERENCES

1. E. Yablonovitch, Photonic crystals, *J Modern Optics* 41 (1994), 173–194.
2. O. Painter, R.K. Lee, A. Scherer, A. Yariv, J.D. O'Brien, P.D. Dapkus, and I. Kim, Two-dimensional photonic band-gap defect mode laser, *Sci* 284 (1999), 1819–1821.
3. S. Olivier, C. Smith, M. Rattier, H. Benisty, C. Weisbuch, T. Krauss, R. Houdre, and U. Oesterle, Miniband transmission in a photonic crystal coupled-resonator optical waveguide, *Optics Lett* 26 (2001), 1019–1021.
4. F. Yang, Y. Qian, R. Coccioli, and T. Itoh, Analysis and application of photonic band-gap (PBG) structure for microwave circuits, *Electromagn* 19 (1999), 241–254.
5. Y. Rahmat-Samii and H. Mosallaei, Electromagnetic band-gap structures: Classification, characterization and applications, *Proc IEEE ICAP Symp* (2001), 560–564.
6. S.-G. Mao, and M.-Y. Chen, A novel periodic electromagnetic bandgap structure for finite-width conductor-backed coplanar waveguides, *IEEE Microwave Wireless Compon Lett* 11 (2001), 261–263.
7. A.R. Weily, L. Horvath, K.P. Esselle, B.C. Sanders, and T.S. Bird, A planar resonator antenna based on a woodpile EBG material, *IEEE Trans Antennas Propagat* 53 (2005), 216–223.
8. L. Yang, M. Fan, F. Chen, J. She, and Z. Feng, A novel compact electromagnetic band-gap (EBG) structure and its application for microwave circuits, *IEEE Trans MTT* 53 (2005), 183–190.
9. A. Erentok, P.L. Lulyak, and R.W. Ziolkowski, Characterization of a volumetric metamaterial realization of an artificial magnetic conductor for antenna applications, *IEEE Trans Antennas Propagat* 53 (2005), 160–172.
10. G. Çakir, Beam-scanning microstrip array antenna design for mobile communication systems: Analytical calculations, computer simulations and measurements, Doctorate thesis, University of Kocaeli, 2004.
11. L. Sevgi, Complex electromagnetic problems and numerical simulation approaches, IEEE Press, Piscataway, NJ, 2003.
12. C. Karpuz, Bandstop characteristics of a triangular microstrip slotted patch as an electromagnetic bandgap (EBG), *Microwave Opt Technol Lett* 36 (2003), 149–150.
13. C. Bowick, RF circuit design, NewNess, Boston, 1982.

© 2005 Wiley Periodicals, Inc.